DOI: 10.1111/jiec.13594

JOURNAL OF INDUSTRIAL ECOLOGY WILEY

RESEARCH ARTICLE

Comparative life cycle assessment of lithium-ion, sodium-ion, and solid-state battery cells for electric vehicles

Florian Degen[1] | Miriam Mitterfellner[1] | Achim Kampker[1,2]

[1]Fraunhofer Research Institution for Battery Cell Production FFB, Münster, Germany

[2]Chair of Production Engineering of E-Mobility Components (PEM) of RWTH Aachen, Aachen, Germany

Correspondence
Florian Degen, Fraunhofer Research Institution for Battery Cell Production FFB, Bergiusstraße 8, 48165 Münster, Germany.
Email: florian.degen@ffb.frauhofer.de

Editor Managing Review: Lynette Cheah

Funding information
Bundesministerium für Bildung und Forschung, Grant/Award Number: 03XP0256

Abstract

The transition toward electrification of transportation has resulted in a rapid increase in the demand for battery cells. While this demand is currently being met through the use of lithium-ion batteries (LIBs), alternative batteries like sodium-ion batteries (SIBs) and solid-state batteries (SSBs) are emerging as relevant alternatives. In this study, we analyze, based on current electric vehicle electrode stack designs, the environmental impact of LIB cells, SIB cells, and SSB cells. The life cycle assessment results from this cradle-to-gate study show that for LIB cell production today, ~58–92 $kgCO_2$-eq are emitted per kWh_{cell} and ~296–624 kWh_{CED}/kWh_{cell} of primary energy is required. In SIB cell production, ~75–87 $kgCO_2$-eq/kWh_{cell} is emitted, and in SSB cell production, ~88–130 $kgCO_2$-eq/kWh_{cell}, depending on their specific electrode stack configuration. The results demonstrate that LFP (lithium–iron–phosphate) cells require the least energy for production across all battery types under analysis. Furthermore, the findings indicate that, in terms of global warming potential (GWP), LFP and NMC900 (nickel–manganese–cobalt) cells are the most sustainable battery types, at least when focusing solely on battery cell production and neglecting subsequent use phases. Furthermore, it is demonstrated that by optimizing the cell designs and their production, the environmental impact of battery cell production can be reduced in the short term by up to −38%. This allows the production of LFP battery cells with a low GWP of ~37 $kgCO_2$-eq/kWh_{cell} and NMC900 cells with ~44 $kgCO_2$-eq/kWh_{cell}. Moreover, there is considerable room for improvement in other major LIB cell types. This article met the requirements for a gold-gold *JIE* data openness badge described at http://jie.click/badges.

KEYWORDS
battery cell production, industrial ecology, life cycle assessment, lithium-ion battery, sodium-ion battery, solid-state battery

1 | INTRODUCTION

The transition from internal combustion engine (ICE) vehicles to electric vehicles (EVs) plays a pivotal role in reducing the global use of fossil fuels and promoting the use of renewable energies. Consequently, the EV market is expanding rapidly, accompanied by a parallel growth in the market for lithium-ion battery (LIB) cells (IEA, International Energy Agency, 2023b). It is anticipated that the demand for battery cells will increase significantly over the next decade. By 2030, the demand is expected to reach 4700 GWh, up from 700 GWh in 2022 (Fleischmann et al., 2023). It is projected that the automotive sector will account for 4300 GWh in 2030, representing 91% of the total battery market (Fleischmann et al., 2023). It is possible that even a demand of 10,000 GWh might be possible by 2040 (Schmaltz et al., 2022).

The future demand for cells will not be met by a single chemistry or configuration but rather by a variety of different chemistries and configurations, as illustrated in Figure 1. Market forecasts indicate that by 2030, the most relevant cathode chemistries will be NMC622, NMC811, NMC900, and LFP (lithium iron phosphate) (Bhandari et al., 2022), with graphite anodes and minor additions of SiO_2 (Link et al., 2023). Other studies concur that NCA (nickel–cobalt–aluminum) will continue to be a relevant cathode material (IEA, International Energy Agency, 2023a). Furthermore, other, novel battery cell types are anticipated to gain market share by 2030 (Bhandari et al., 2022; IEA, International Energy Agency, 2023a). This may encompass sodium-ion batteries (SIBs), solid-state batteries (SSBs), or other cell chemistries. In addition to the cell chemistry itself, the corresponding cell configuration is also relevant. Almost any cell chemistry can be applied in battery cells with either a high-power (HP) configuration or a high-energy (HE) configuration, depending on the type of EV in question (Lain et al., 2019; Link et al., 2023).

Cells with HP configurations are capable of facilitating high charge and discharge currents, although they exhibit a reduced energy storage capacity. This is particularly pertinent to EVs with high sudden power demand, such as hybrid vehicles (Link et al., 2023), battery electric sports cars, or heavy-duty vehicles. This is achieved by reducing the thickness of the active material layer on the anode and cathode sides, thereby minimizing the electric, ionic, and thermal resistance (Ding et al., 2019; Rauscher, 2014). Conversely, a particularly thick layer of active material with the same cell chemistry leads to a HE configuration of the battery cell (Lain et al., 2019). This implies that the possible charge and discharge rates are lower, yet the energy storage capacity is higher (Ding et al., 2019; Masias et al., 2021). This type of cell is employed especially in EVs with a particularly extended range (Link et al., 2023). According to a meta-study conducted by Link et al. (2023), more than 67% of the battery cells in EVs between 2016 and 2022 exhibited a cathode layer thickness between approximately 50 µm (HP configuration) and 90 µm (HE configuration).

Multiple studies in the past have dealt with life cycle assessment (LCA) of battery cell production to understand a variety of their impacts, such as energy consumption and greenhouse gas (GHG) emissions (see Supplement S4 for an overview about existing LCA studies on LIB cells) (Ambrose & Kendall, 2016; Bawankar et al., 2023; Crenna et al., 2021; Cusenza et al., 2019; Dai et al., 2019; Deng et al., 2017; Ellingsen et al., 2014; Faria et al., 2014; Gutsch & Leker, 2024; Jenu et al., 2020; Kallitsis et al., 2020; Kim et al., 2016; Le Varlet et al., 2020; Majeau-Bettez et al., 2011; Marques et al., 2019; Notter et al., 2010; Qian et al., 2023; Shen et al., 2023; Sun et al., 2020; Winjobi et al., 2022; Zackrisson et al., 2010; Zhao & You, 2019). Broadly, these studies have highlighted the prominence of energy-intensive battery cell production (Degen & Schütte, 2022; Kallitsis, 2022) and the environmental impact of the used material (Gutsch & Leker, 2024). Llamas-Orozco et al. evaluate the life cycle impacts of all major LIB chemistries—both NMC (nickel–manganese–cobalt; NMC111, NMC532, NMC622, NMC811, and NMC900) and LFP (Llamas-Orozco et al., 2023). This remains the only study to date to evaluate all LIB-relevant chemistries. However, it does not evaluate the life cycle impacts of SIBs and SSBs.

The most relevant LCA studies of SIB cells are those by Peters et al. (2016), Schneider et al. (2019), and Peters et al. (2021). Relevant LCA studies of SSB cells are those by Keshavarzmohammadian et al. (2018); Lastoskie & Dai (2015); Smith et al. (2021); Troy et al. (2016); Zhang et al. (2022). The SSB-related studies exclusively evaluate small SSB coin cells with a low technology readiness level (Mandade et al., 2023). The results are therefore difficult to extrapolate to large cells on a kWh scale. It should also be noted that SIB, SSB, and LIB are collective terms for general battery cell classes, which can be divided into subclasses, like NMC, NCA, and LFP for LIB battery cells. Each of these specific subclasses exhibits distinct properties and environmental impacts.

However, in the majority of LCA studies of LIBs, no distinction is made between HP and HE cell configurations that are relevant to the application in EVs. Additionally, the aforementioned studies do not account for the effect of the latest trends in the LIB industry that affect the battery design, such as reducing the thickness of current collectors, the use of water as the solvent, and the adaptation of anodes for dry coating. This results in an incomplete understanding of the resultant life cycle impacts of batteries. Furthermore, these studies concentrate almost exclusively on the impact category of global warming potential (GWP), while other impacts, such as eutrophication and toxicity, are largely overlooked. Consequently, the objective of this study is to ascertain the environmental impact of battery cell types and designs currently in use and those anticipated to be employed in the near future within the automotive industry, from the point of production to the point of entry into the supply chain.

The study differs from existing literature and enhances this regarding the following points:

- All LIB cell chemistries are considered and compared in one single study, which is relevant for EVs (NCA, NMC532, NMC622, NMC811, NMC900, and LFP).
- Dedicated cell designs are developed and used for the LCA, based on existing EV batteries, to ensure comparability and proximity to reality.
- A distinction is made between HE and HP cell configurations, as this is common in EV applications.

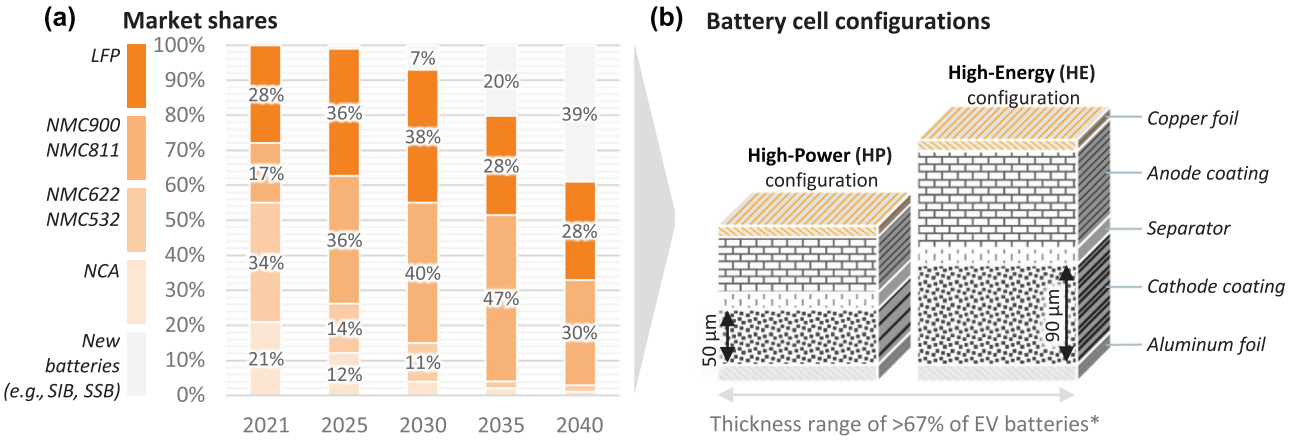

FIGURE 1 Forecasted market shares of cell chemistries (Bhandari et al., 2022) (a) and their practical configuration range (Link et al., 2023) (b). The dimensions of the electrode stacks are shown to scale for the high-power (HP) configuration and high-energy (HE) configuration of an NMC622 cell with 100% graphite anode. *For the years 2016–2022, based on $n = 72$ battery tear downs (Link et al., 2023). EV, electric vehicle; LFP, lithium–iron–phosphate; NMC, nickel–manganese–cobalt; NCA, nickel–cobalt–aluminum; SIB, sodium-ion battery; SSB, solid-state battery.

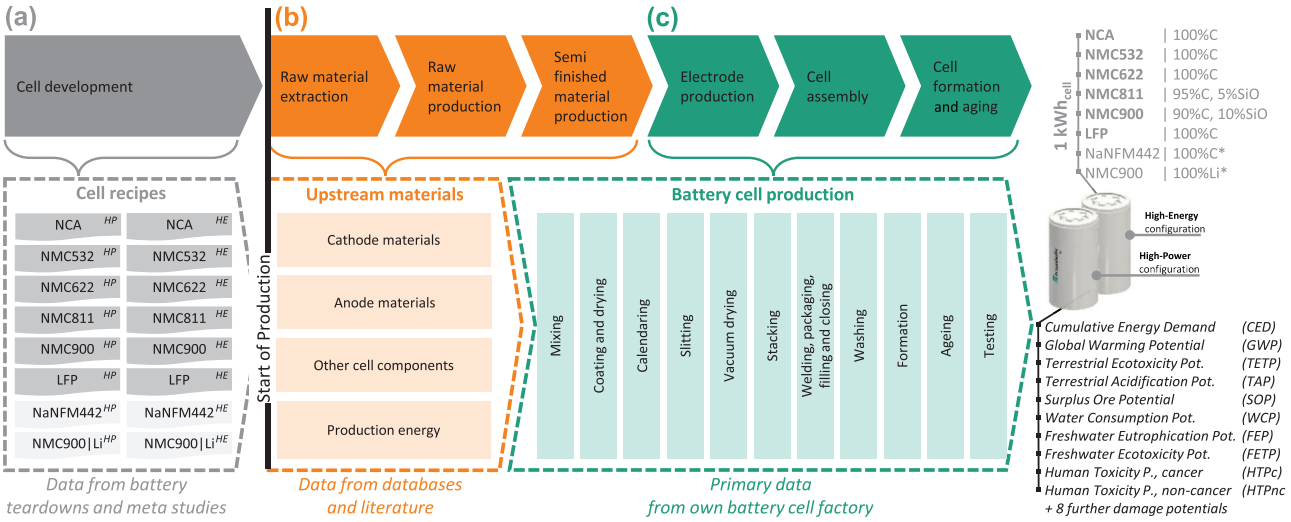

FIGURE 2 System boundaries of life cycle assessment (LCA) study and used data sources. Assessed battery cell designs and recipes (a), assessed material flows (b), and assessed production steps (c). In total 18 environmental impact criteria are assessed, for most of today's common six cell chemistries in EVs, in two configurations each, from cradle to gate. For this, primary data from battery teardowns, from literature, from databases, and from an own battery cell factory are used. Pot., potential.

- Future cell chemistries such as SIB cells and SSB cells are also considered in the study, based on the same databases and cell designs, to be able to put this into context with today's LIB cells.
- The entire material value chain is analyzed in detail, including the synthesis of cathode active material (CAM).
- Own primary data from a battery cell factory are used for this study.
- All 18 ReCiPe impact criteria are analyzed, not just GWP or cumulative energy demand (CED) like in many other studies.
- Uncertainties in the material data are quantitatively taken into account and explicitly shown.
- Development trends in cell design and cell recipes are analyzed to determine their future effect on the environmental impact of battery cells.

2 | METHODS

In this study, a cradle-to-gate LCA is conducted. Figure 2 shows the system boundaries of this LCA and where data are obtained from. Based on teardowns of commercial EV LIBs (A2Mac1, 2023; B3 Corporation, 2015; Quinn et al., 2018) and meta-studies (Link et al., 2023), a team of cell

designers designed cell recipes for all current chemistries (NCA, NMC532, NMC622, NMC811, NMC900) and near-future chemistries (sodium-ion: NaNFM442, solid-state: NMC900|Li with oxidic electrolyte), once for HP cells and once for HE cells (A).

For SIBs, NaNFM442 is employed as representative cathode chemistry, as NaNFP442 exhibits comparatively favorable energy densities, a low nickel content, and, most importantly, can be synthesized with existing equipment. In particular, large-scale synthesis is a prerequisite for large-scale use in EV batteries. Nevertheless, other SIB chemistries can also be used in EVs in the future. For SSBs, we employ NMC900 as the cathode chemistry, with oxide solid electrolyte (SE). The choice of NMC900 is motivated by its exceptionally HE densities, comparable to those of lithium metal on the anode side. The selection of oxide solid-state electrolytes is driven by the likelihood of their industrialization on a large scale (Schmaltz et al., 2022). It is also possible that other SSB chemistries may be employed in EVs in the future.

For the defined cells, the cell recipes and the specific bill of materials (BOM) were then created as well as the corresponding life cycle inventory (LCI). Through our access to our own battery cell factory, we were then able to expand the material-specific LCI with our own primary data to include the battery cell production. At the end of the analysis, we obtain the environmental damage potentials CED, GWP, terrestrial ecotoxicity potential (TETP), terrestrial acidification potential (TAP), surplus ore potential (SOP), water consumption potential (WCP), freshwater eutrophication potential (FEP), freshwater ecotoxicity potential (FETP), human toxicity potential, cancer (HTPc), and human toxicity potential, non-cancer (HTPnc). For the most common six cell chemistries, in two configurations, each of these 10 environmental damage potentials are calculated and assessed. The remaining environmental damage potentials are shown in Supplement S4. The calculation formulae, assumptions, and further details are provided in Supplement S1.

3 | RESULTS

3.1 | Design and recipes of electrode stacks

The most commonly used EV LIB cathode chemistries are NCA, NMC532, NMC622, NMC811, and LFP, with graphite being the anode (Bhandari et al., 2022; IEA, International Energy Agency, 2023a; Link et al., 2023). Modern NMC811 chemistries use graphite anodes that are blended with a small amount of SiO. Nickel-rich cathodes, such as NMC900, are gaining ground in EV batteries and are likely to witness a major increase in their usage in this domain (Bhandari et al., 2022). In theory, for each of these chemistries, cells of both HE and HP cell configurations can be manufactured. However, in practice, some chemistry-configuration combinations are more preferred than others. For example, NMC chemistries are used in both HE and HP configurations, while LFP is almost exclusively produced in HE configuration (Link et al., 2023). Since many battery manufacturers have announced the emergence and introduction of SIBs and SSBs in EVs by the end of this decade, we also include these batteries in this analysis. Figure 3 shows the designed battery cells, respectively their electrode stacks, their specifications, and their respective BOM. The electrode stack is hereby the battery cell without casing.

To facilitate comparison, a constant cathode thickness was defined as a reference variable for both an HP and an HE configuration. In accordance with the meta-study by Link et al., for the HP configuration, a calendared cathode thickness of 50 µm and porosity of 35% was selected as the upper limit, while for the HE configuration, a calendared cathode thickness of 90 µm and porosity of 27% was chosen as the upper limit (Link et al., 2023). The average thickness of the current collectors and the separator is also provided by Link et al. (2023). All other variables are derived from these numbers. For the SIB cells and SSB cells, the parameters of the LIB cells were adopted as applicable. The BOM indicates that a distinction between the HE and HP configurations does affect the mass of the passivating material per kWh_{cell} but not the mass of the active material.

3.2 | Material flows along the upstream value chain

The environmental impact of the material in a battery cell has a significant contribution to the environmental impact of the entire final battery cell. Figure 4 shows the material flow along the value chain for NCA, NMC811, LFP, NaNFM442 (SIB), and NMC900|Li (SSB) battery cells in an HE configuration, starting from the inputs for CAM precursor synthesis, for each 1 kWh_{cell} of battery cell energy storage capacity. The material flow diagrams for NMC532, NMC622, and NMC900 in HE configurations can be found in Supplement S4. The material flow values for HP configurations can be found in Supplement S2.

Figure 4 illustrates that the production of an LIB cell capable of storing 1 kWh of energy requires between ~3.2 kg (for NMC900) and ~5.2 kg (for LFP) of material. While Li_2CO_3 is the standard lithium source for the majority of CAMs, LiOH is employed for nickel-rich chemistries (Dai et al., 2018), such as NCA, NMC811, or NMC900, which is usually obtained from Li_2CO_3. The production of the precursor is carried out hydrothermally (Dai et al., 2018; Dunn et al., 2015). The CAM with nickel content is produced by solid-state synthesis (Dai et al., 2018; Dunn et al., 2015). Given that LFP can be produced both hydrothermally and by solid-state synthesis (Dunn et al., 2015), we have also elected to utilize solid-state synthesis for LFP, thereby ensuring greater comparability. Additionally, for NaNFM442 (SIB), a hydrothermally produced precursor is employed, followed by solid-state synthesis. The Na source is Na_2CO_3.

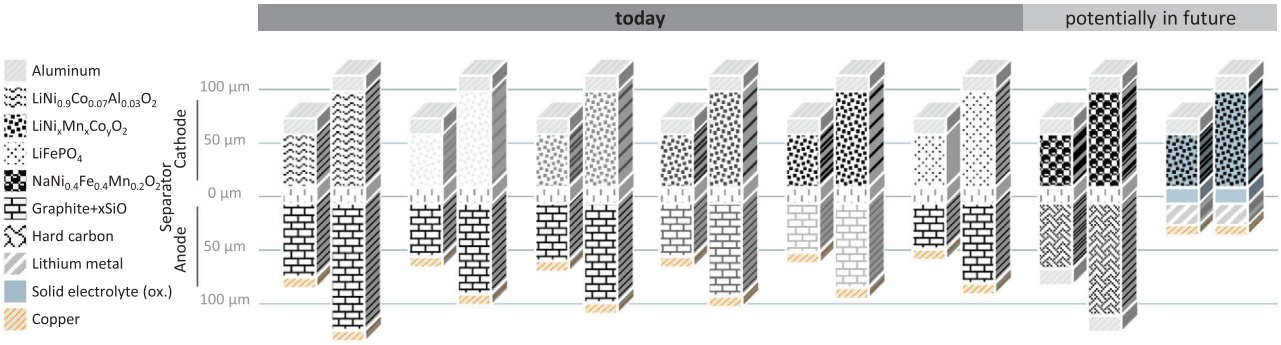

		NCA		NMC532		NMC622		NMC811		NMC900		LFP		NaNFM442 (SIB)		NMC900 (SSB)	
General	Cell configuration	High Power	High Energy	High Power	High Energy	High Power	High Energy	High Power	High Energy	High Power	High Energy	High Power	High Energy	High Power*	High Energy*	High Power*	High Energy*
	Cell voltage (V)	3.60		3.60		3.60		3.60		3.60		3.20		3.00		3.70	
	Areal energy of mono stack (kWh/m²)	0.22	0.42	0.17	0.32	0.17	0.33	0.20	0.40	0.23	0.44	0.12	0.24	0.11	0.21	0.23	0.45
	Gravim. weight of 1 m² mono stack (kg/m²)	0.93	1.51	0.86	1.38	0.87	1.40	0.85	1.36	0.82	1.32	0.75	1.18	0.76	1.22	0.65	1.05
	Gravim. energy density of stack (kWh/kg)	0.23	0.28	0.19	0.23	0.20	0.24	0.24	0.29	0.27	0.33	0.16	0.20	0.14	0.17	0.36	0.43
	Reference: capcacity per 4680 cell (Ah)	23.3	28.3	20.5	25.1	20.4	24.9	25.0	30.6	28.8	35.4	17.8	21.9	14.3	17.5	36.7	50.7
Cathode	Active material	NCA		NMC532		NMC622		NMC811		NMC900		LFP		NaNFM422		NMC900	
	Formula	$Li_1Ni_{0.9}Co_{0.07}Al_{0.03}O_2$		$Li_1Ni_{0.5}Mn_{0.3}Co_{0.2}O_2$		$Li_1Ni_{0.6}Mn_{0.2}Co_{0.2}O_2$		$Li_1Ni_{0.8}Mn_{0.1}Co_{0.1}O_2$		$Li_1Ni_{0.9}Mn_{0.05}Co_{0.05}O_2$		$Li_1Fe_1P_1O_4$		$Na_1Ni_{0.4}Fe_{0.4}Mn_{0.2}O_2$		$Li_1Ni_{0.9}Mn_{0.05}Co_{0.05}O_2$	
	Ratio active mat./binder/carbon black (%)	93/3/4		93/3/4		93/3/4		93/3/4		93/3/4		93/3/4		93/3/4		93/3/4	
	Thickness active mat. calendered (µm)	**50**	**90**	**50**	**90**	**50**	**90**	**50**	**90**	**50**	**90**	**50**	**90**	**50**	**90**	**50**	**90**
	Porosity after calendering (%)	31	25	31	25	31	25	31	25	31	25	31	25	31	25	31	25
	Thickness of current collector Al (µm)	15		15		15		15		15		15		15		15	
	Specific energy of active material (mAh/g)	206		154		158		190		210		160		135		210	
Anode	Active material	Graphite		Graphite		Graphite		Graphite, 5%SiO		Graphite, 10%SiO		Graphite		Hard carbon		Lithium metal	
	Ratio active mat./binder/carbon bl. (%)	94/2/4	95/1/4	94/2/4	95/1/4	94/2/5	95/1/5	94/2/6	95/1/6	94/2/7	95/1/7	94/2/8	95/1/8	94/2/8	95/1/8	100/0/0	100/0/0
	Thickness active mat. calendered (µm)	69	119	52	90	54	93	50	87	46	79	44	75	61	105	20	20
	Porosity after calendering (%)	35	27	35	27	35	27	35	27	35	27	35	27	35	27	0	0
	Thickness of current collector Cu* (µm)	10		10		10		10		10		10		15		10	
	Specific energy of active material (mAh/g)	360		360		360		462		564		360		350		3860	
	Thickness of separator/SE (µm)	15		15		15		15		15		15		15		15	
Bill of materials (BOM)	Mass Li in CAM (g/kWh$_{cell}$)	97		130		126		104		94		86				94	
	Mass Na in CAM (g/kWh$_{cell}$)													508			
	Mass Ni in CAM (g/kWh$_{cell}$)	737		548		639		706		717				519		717	
	Mass Mn in CAM (g/kWh$_{cell}$)			308		199		83		37				243		37	
	Mass Co in CAM (g/kWh$_{cell}$)	58		220		214		89		40						40	
	Mass Al in CAM (g/kWh$_{cell}$)	11															
	Mass Fe in CAM (g/kWh$_{cell}$)											691		493			
	Mass P in CAM (g/kWh$_{cell}$)											383					
	Mass O in CAM (g/kWh$_{cell}$)	446		598		580		481		434		792		707		434	
	Mass binder cathode (g/kWh$_{cell}$)	43		58		57		47		43		63		80		42	
	Mass carbon black cathode (g/kWh$_{cell}$)	58		78		76		63		57		84		106		55	
	Mass graphite (g/kWh$_{cell}$)	849		849		849		628		488		955					
	Mass SiO (g/kWh$_{cell}$)							33		54							
	Mass hard carbon (g/kWh$_{cell}$)													1048			
	Mass lithium metal (g/kWh$_{cell}$)															864	442
	Mass binder anode (g/kWh$_{cell}$)	36	36	36	36	36	36	28	28	23	23	41	40	45	44		
	Mass carbon black anode (g/kWh$_{cell}$)	18	9	18	9	18	9	14	7	12	6	20	10	22	11		
	Mass electrolyte/SE (g/kWh$_{cell}$)	672	449	778	519	765	510	622	414	540	360	978	651	1291	863	576	384
	Mass aluminum foil (g/kWh$_{cell}$)	187	95	245	125	238	122	199	102	180	92	332	170	381	195	175	89
	Mass copper foil (g/kWh$_{cell}$)	411	210	540	276	524	268	439	224	396	202	732	374			385	197
	Mass separator (g/kWh$_{cell}$)	207	106	272	139	264	135	221	113	200	102	369	189	424	217		
	Mass Fe-casing (g/kWh$_{cell}$)	560	461	638	521	641	525	522	426	453	369	824	670	1093	895	346	251

FIGURE 3 Stack designs and bill of materials of current lithium-ion battery (LIB) cells in electric vehicles (EVs). The cells are designed based on product teardowns of automotive battery cells (A2Mac1, 2023; Quinn et al., 2018), on battery databases (Fraunhofer Institute for Systems & Innovation Research ISI, 2023), and on meta-studies that investigate automotive battery cell designs between 2016 and 2022 (Link et al., 2023); >67% of the analyzed LIB cells in EVs have a cathode coating thickness between 50 µm (high-power [HP] configuration) and 90 µm (high-energy [HE] configuration), ($n = 75$) (Link et al., 2023). Calculations and further details can be found in Supplement S2. We use $Li_{1.3}Al_{0.3}Ti_{1.7}(PO_4)_3$ as a solid electrolyte for the solid-state battery (SSB) cell. *Whether a distinction between HP and HE cells will be made with sodium-ion batteries (SIBs) and SSB in the future is unknown, but for better comparability, we designed both chemistries once in an HP and once in an HE configuration. LFP, lithium–iron–phosphate; NCA, nickel–cobalt–aluminum; NMC, nickel–manganese–cobalt.

It is notable that approximately twice as much mass is required as input as the mass of a battery cell results as output. Consequently, during synthesis and production, by-products and waste are created, in particular, sodium sulfate ($NaSO_4$) during precursor production and N-methyl-2-pyrrolidone (NMP, respectively, C_5H_9NO), during electrode production. The sodium sulfate can be employed in other industrial processes, while the NMP can either be reconditioned or combusted (Ahmed et al., 2016). By-products and waste, respectively their environmental impacts, are not allocated to the LCI. Thus, their environmental impacts are also not allocated to the battery cells.

3.3 | Environmental impact of the input materials and the final battery cell

Each of the materials utilized in the production of the battery and its constituent components have distinct environmental impacts. Figure 5 illustrates the environmental impact of the input materials per kilogram for the categories CED, GWP, TETP, TAP, SOP, WCP, FEP, FETP, HTPc, and

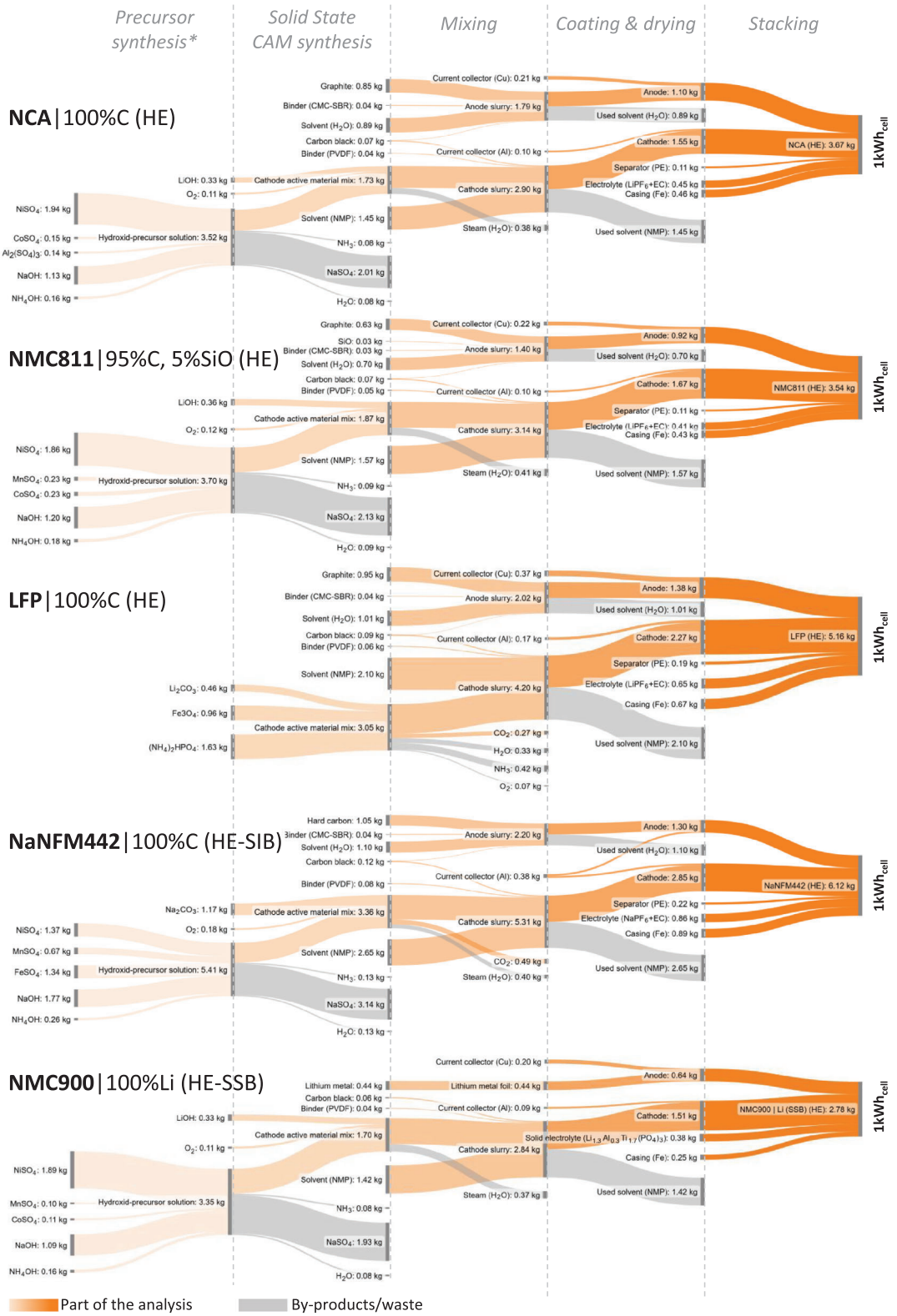

FIGURE 4 Material flow along the upstream value chain, starting with the material input for precursor synthesis, to produce a battery cell of 1 kWh_{cell} energy storage capacity. The material flows shown here are for battery cells in high-energy (HE) configuration. The material flows for NMC532, NMC622, and NMC900 are shown in Supplement S4. Data for the HP configuration can be found in Supplement S2. *The circular flow of water (H_2O), which is used as a solvent during the precursor synthesis, is not shown here for better readability. NMC, nickel–manganese–cobalt; LFP, lithium–iron–phosphate; NCA, nickel–cobalt–aluminum; SSB, solid-state battery; SIB, sodium-ion battery.

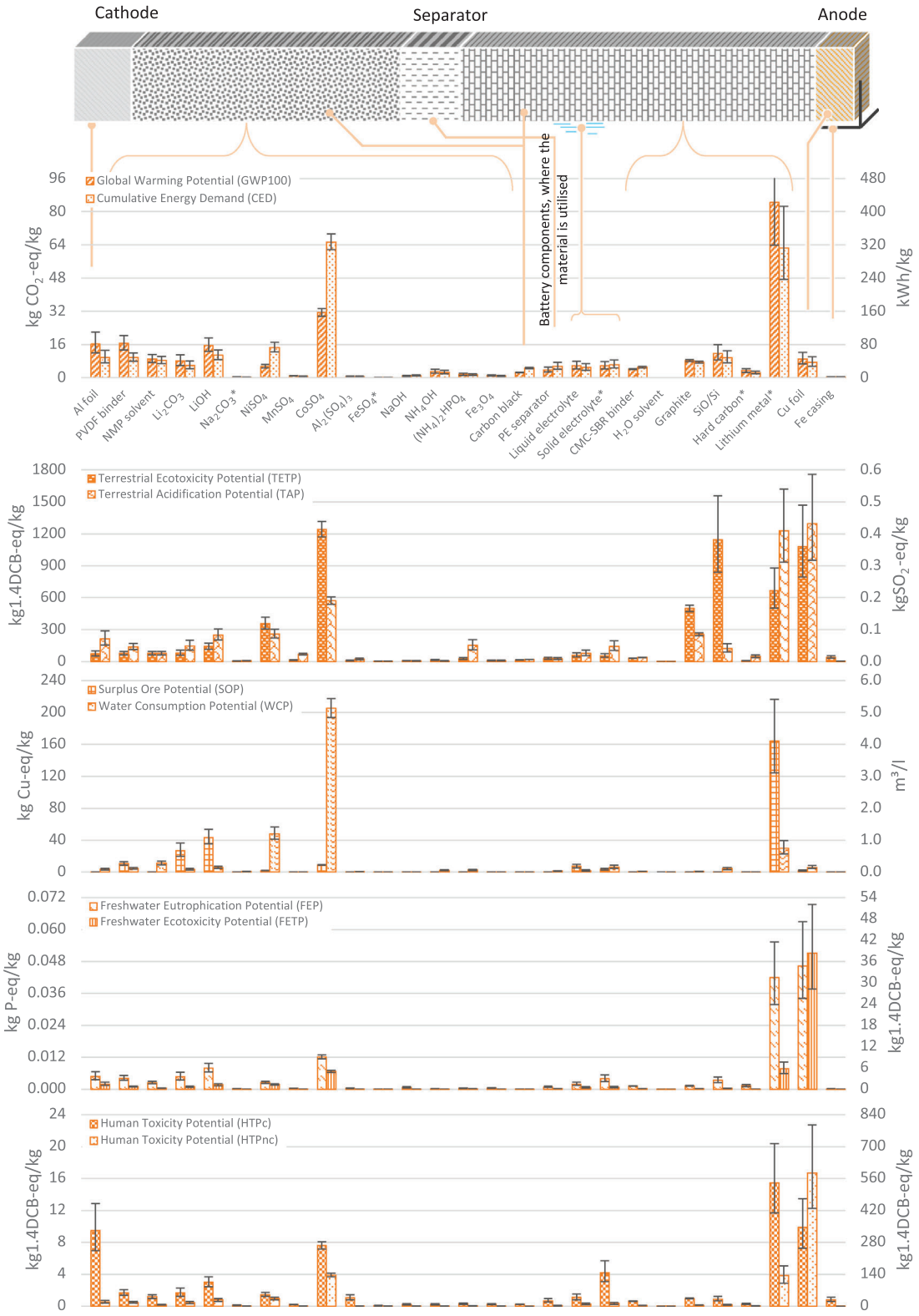

FIGURE 5 Environmental impact of battery materials per kilogram. The mass per specific cell chemistries varies and is defined by the cell-specific bill of materials. The data are from Ecoinvent 3.10 database and were calculated using the ReCiPe2016 v1.03 (H) method (Huijbregts et al., 2016). The data have a log-normal distribution. The error bars show the 67% confidence interval. The corresponding data can be found in Supplement S2. *Material that is required for SIB or SSB cells. SSB, solid-state battery; SIB, sodium-ion battery.

HTPnc. The environmental impact of the remaining eight categories can be found in Supplement S4. The data were calculated using the ReCiPe2016 v1.03 (H) method (Huijbregts et al., 2016), based on the Ecoinvent database version 3.10.

Figure 5 illustrates that in terms of the GWP of LIB cells, cobalt sulfate ($CoSO_4$) has the most significant impact, with a value of approximately 31 $kgCO_2eq/kg$. In contrast, nickel, in the form of nickel sulfate ($NiSO_4$), which represents the largest weight share in most nickel-based cell chemistries, has a relatively moderate GWP of approximately 5 $kgCO_2eq/kg$. It is noteworthy that the GWP of diammonium phosphate ($(NH_4)_2HPO_4$) and magnetite (Fe_3O_4) is relatively low. Both are essential raw materials for the production of LFP batteries. The reason for this is that ($(NH_4)_2HPO_4$) has been produced on a large scale for many decades, namely as fertilizers. Economies of scale, learning effects, and lower energy consumption, which consequently result in a lower GWP, can be achieved through the application of these principles. In contrast, Fe_3O_4 is a mineral that is widely available in nature and is used in many industries. For SSB cells, lithium metal is used, which has the highest GWP (~84 $kgCO_2eq/kg$). To obtain 1 kg of Li, approximately 7 kg of LiCl is processed by electrolysis, requiring approximately 30 kWh of electricity, which is obtained by combustion of hard coal and natural gas.

With regard to the CED, $CoSO_4$ stands out in particular due to its high CED, as illustrated in Figure 5. It can be observed that approximately 327 kWh_{CED} of energy is required to produce 1 kg of $CoSO_4$. In comparison, 1 kg of $NiSO_4$, the input material with the second highest CED for LIB cells, requires 73 kWh_{CED}. The results are similar for the other active categories. In this context, it is evident that $CoSO_4$ and $NiSO_4$ represent the primary sources of environmental damage potential, in addition to Li metal for SSB cells. However, it is noteworthy that the copper foil also exhibits a considerable degree of environmental impact, particularly in the domains of toxicity, acidification, and eutrophication. In this regard, copper is arguably as critical as cobalt, respectively $CoSO_4$. Furthermore, it is important to highlight that the choice of lithium source can have a significant impact on the overall environmental footprint. It is evident that LiOH exhibits a markedly elevated degree of environmental damage potential in comparison to Li_2CO_3. However, it should be noted that the values for Li_2CO_3, LiOH, and graphite from Ecoinvent are challenged in the literature. A review of the literature by Engels et al. (2022) indicates that the GWP of natural graphite is likely to be 9.6 kg CO_2 eq/kg, which is approximately four times higher than the Ecoinvent data from 2020 (Engels et al., 2022). A review of the literature by Rolinck et al. indicates that in the most significant LCA studies on Li_2CO_3 and LiOH, the GWP of Li_2CO_3 is, on average, approximately 6 $kgCO_2eq/kg$, while that of LiOH is approximately 12 $kgCO_2eq/kg$ (Rolinck et al., 2023). For this reason, a sensitivity analysis was conducted to investigate the impact of changes in base values, such as those derived from literature sources, on the overall impact of an entire battery cell. The results pertaining to GWP can be found in Supplement S4. The results demonstrate that alterations to the base values of Li_2CO_3, LiOH, and graphite result in only a marginal change in the GWP of a complete battery cell. Furthermore, there is no evidence to suggest that there are significant discrepancies in the base values, at least not from the most recent data from Ecoinvent 3.10. Given these considerations and the need for consistency, we will continue to utilize the values from Ecoinvent 3.10 in the subsequent analyses.

Figure 6 shows the CED and GWP of the different cell chemistries, respectively, battery cells in HP configuration and HE configuration. The figure demonstrates that there is a notable distinction between the CED of cell chemistry produced in an HE or HP configuration. The HP configuration exhibits a CED that is approximately 6%–17% higher than the respective HE configuration. It also can be observed that the NMC532 and the NMC622 chemistries have the highest CED (NMC582: ~582–620 kWh_{CED}/kWh_{cell}, NMC622: ~587–624 kWh_{CED}/kWh_{cell}). NMC900 has the lowest CED among the LIB chemistries with nickel content; NMC811 and NCA are in between (NMC900: ~390–418 kWh_{CED}/kWh_{cell}, NMC811: ~454–484 kWh_{CED}/kWh_{cell}, NCA: 427–456 kWh_{CED}/kWh_{cell}). LFP cells have by far the lowest CED of all the chemistries analyzed (LFP: ~296–346 kWh_{CED}/kWh_{cell}). Also, SIB cells, often promoted as sustainable alternatives to LIB cells, have a CED that is notably higher than the CED of LFP cells (SIB: ~441–493 kWh_{CED}/kWh_{cell}). The reason is, that also in NaNFM442 nickel, respectively $NiSO_4$ is used, which has a high CED. Also, oxidic SSB cells have a high CED (~493–655 kWh_{CED}/kWh_{cell}). The reason for this is the high CED of lithium metal that is used as an anode material. However, it can be observed that what all LIB chemistries have in common is that the majority of the CED is caused by the material itself (~78–92%), with the energy in battery cell production accounting for a relatively smaller proportion (~8%–22%). The main CED driver is the cathode slurry. In the case of nickel-based cathode slurries, this is, in particular, the $CoSO_4$, the $NiSO_4$, and the solvent NMP. The CED contribution of Li_2CO_3, LiOH, and other components is low. It is noteworthy that the NMP makes up more than 50% of the CED in the LFP slurries.

A qualitatively similar picture emerges for the GWP. Here, the nickel-based LIB chemistries have a GWP between ~57 and 92 $kgCO_2$-eq/kWh_{cell}, while LFP cells have a GWP of ~59–70 $kgCO_2$-eq/kWh_{cell}. While for CED, LFP is the chemistry with the lowest impact, in terms of GWP, NMC900 cells have the lowest GWP, with ~57 $kgCO_2$-eq/kWh_{cell}. Furthermore, SIB cells and SSB cells have a GWP that is notably higher than that of all analyzed LIB cells.

Figure 7 illustrates the various impact categories and their respective environmental damage potentials, namely TETP, TAP, SOP, WCP, FEP, FETP, HTPc, and HTPnc, for the different cell chemistries and configurations. The results for the remaining eight damage potentials can be found in Supplement S4. A similar picture emerges when considering the environmental and human health damage potential of cobalt and $CoSO_4$. The lower the concentration of cobalt, the better it is for the environment and humans. Likewise, LFP and NaNFM422 (SIB) are the chemistries with the lowest damage potential in almost all impact categories. It is notable that, in addition to the cathode slurry, the copper foil is the battery component with the highest damage potential. This has a particularly strong effect on LFP cells, where the copper foil has the largest damage potential in all impact categories except WCP. For SIB cells, this is beneficial, as aluminum is used on the anode side as a current collector, instead of copper.

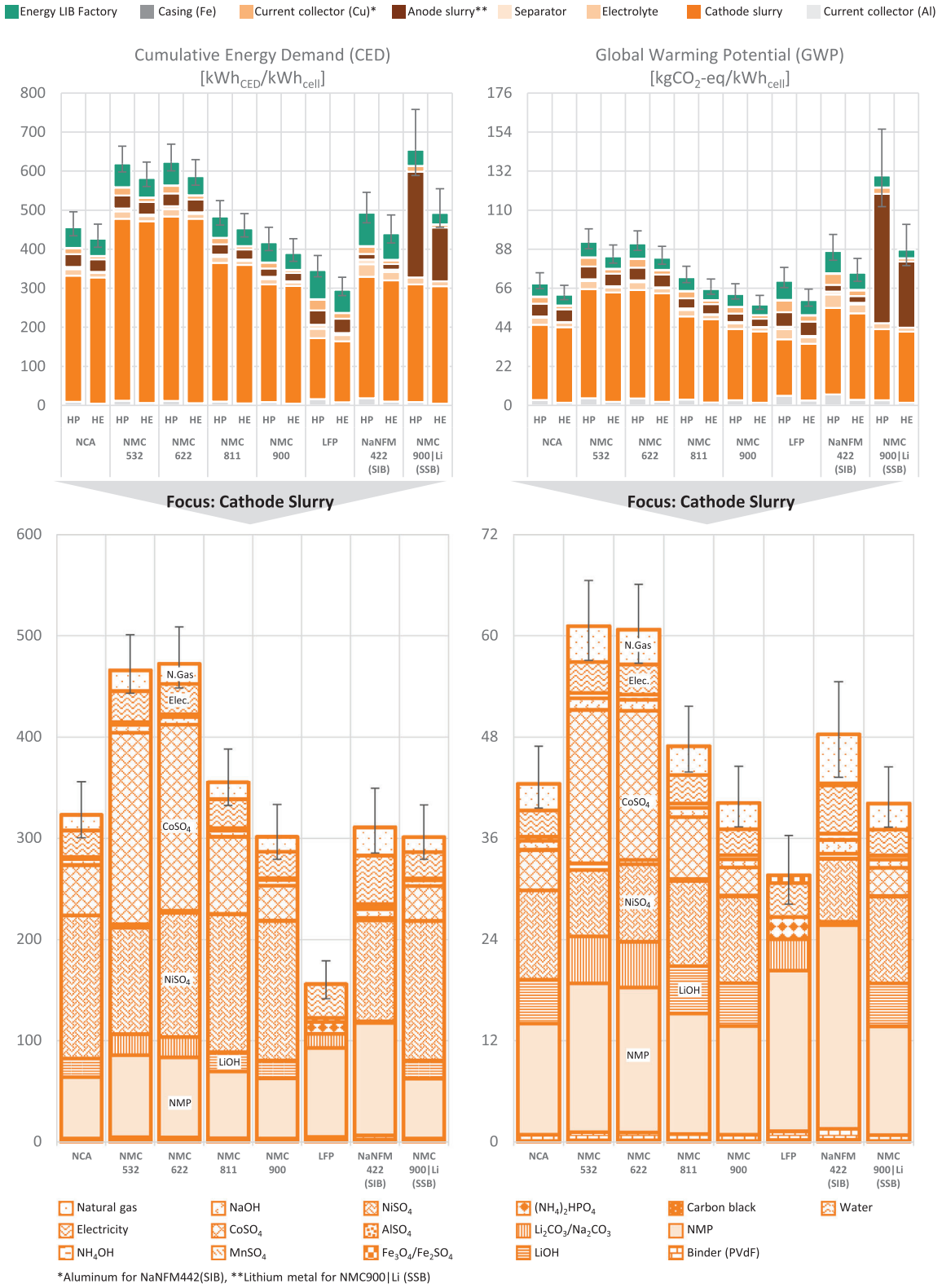

FIGURE 6 Cumulative energy demand (CED) and global warming potential (GWP) of different battery cell chemistries, in different configurations. The corresponding data can be found in Supplement S2. The data have a log-normal distribution. The error bars show the approximated 67% confidence interval. NMP, N-methyl-2-pyrrolidone; NMC, nickel–manganese–cobalt; LFP, lithium–iron–phosphate; NCA, nickel–cobalt–aluminum; SSB, solid-state battery; SIB, sodium-ion battery.

FIGURE 7 Environmental impact of different LIB chemistries, in different configurations. The corresponding data can be found in Supplement S2. The data have a log-normal distribution. The error bars show the approximated 67% confidence interval. HE, high energy; HP, high power; NMC, nickel–manganese–cobalt; LFP, lithium–iron–phosphate; NCA, nickel–cobalt–aluminum.

Highest value within each column

Average value within each column

Lowest value within each column

		Cumulative Energy Demand (CED) [kWh/kWh]	Global Warming Potential (GWP) [$kgCO_2$-eq/kWh]	Terrestrial Ecotoxicity Potential (TEP) [kg1.4DCB-eq/kWh]	Terrestrial Acidification Potential (TAP) [$kgSO_2$-eq/kWh]	Surplus Ore Potential (SOP) [kgCu-eq/kWh]	Water Consumption Potential (WCP) [m^3/kWh]	Freshwater Eutrophication Potential (FEP) [kg P-eq/kWh]	Freshwater Ecotoxicity Potential (FEtP) [kg1.4DCB-eq/kWh]	Human toxicity, cancer (HTPc) [kg1.4DCB-eq/kWh]	Human toxicity, non-cancer (HTPnc) [kg1.4DCB-eq/kWh]
Base scenario	NCA (HE)	426.9	62.3	1820	0.5	24.7	3.8	0.033	13.3	13.4	253
	NMC532 (HE)	583.4	84.1	2343	0.6	32.4	5.6	0.044	18.3	18.3	353
	NMC622 (HE)	587.7	83.3	2369	0.6	32.1	5.8	0.043	17.6	18.0	343
	NMC811 (HE)	453.4	65.5	1851	0.5	26.2	4.2	0.035	14.2	14.0	271
	NMC900 (HE)	390.4	56.8	1603	0.4	23.1	3.5	0.031	12.6	12.1	238
	LFP (HE)	296.3	59.3	1281	0.5	19.0	1.0	0.038	16.8	13.3	275
NMP recycling	NCA (HE)	379.3	50.9	1715	0.4	24.6	3.4	0.030	12.9	11.8	244
	NMC532 (HE)	519.8	68.9	2203	0.6	32.3	5.1	0.041	17.8	16.1	341
	NMC622 (HE)	525.6	68.4	2232	0.6	32.0	5.3	0.040	17.1	15.9	332
	NMC811 (HE)	401.9	53.2	1737	0.5	26.1	3.8	0.032	13.7	12.3	261
	NMC900 (HE)	343.7	45.6	1500	0.4	23.0	3.1	0.029	12.2	10.5	229
	LFP (HE)	227.4	42.8	1129	0.4	18.9	0.5	0.034	16.2	11.0	262
Thickness reduction of current collector (Al & Cu)	NCA (HE)	422.2	61.0	1727	0.4	24.5	3.8	0.029	10.0	11.8	204
	NMC532 (HE)	577.3	82.5	2214	0.5	32.2	5.6	0.038	13.8	16.3	284
	NMC622 (HE)	581.7	81.6	2250	0.5	31.9	5.7	0.038	13.4	16.1	280
	NMC811 (HE)	448.4	64.2	1751	0.4	26.0	4.1	0.031	10.7	12.4	218
	NMC900 (HE)	385.8	55.6	1513	0.4	22.9	3.5	0.027	9.4	10.7	190
	LFP (HE)	287.9	57.0	1115	0.4	18.7	1.0	0.030	10.9	10.7	187
LIB-factory: optimized production*	NCA (HE)	419.4	61.0	1814	0.5	24.7	3.8	0.033	13.2	13.2	253
	NMC532 (HE)	578.4	83.2	2342	0.6	32.6	5.6	0.044	18.4	18.3	354
	NMC622 (HE)	580.2	81.9	2364	0.6	32.1	5.8	0.043	17.6	17.9	343
	NMC811 (HE)	446.2	64.2	1846	0.5	26.2	4.2	0.035	14.1	13.9	271
	NMC900 (HE)	383.4	55.6	1599	0.4	23.1	3.5	0.031	12.5	12.0	237
	LFP (HE)	273.4	55.6	1267	0.5	19.0	1.0	0.036	16.7	13.0	274
LIB-factory: electricity instead of natural gas	NCA (HE)	429.6	61.8	1819	0.5	24.7	3.8	0.034	13.3	13.3	255
	NMC532 (HE)	590.2	84.1	2348	0.6	32.6	5.6	0.046	18.4	18.5	356
	NMC622 (HE)	591.5	82.7	2370	0.6	32.1	5.8	0.044	17.6	18.1	345
	NMC811 (HE)	456.7	65.1	1851	0.5	26.2	4.2	0.036	14.2	14.1	273
	NMC900 (HE)	393.4	56.4	1604	0.4	23.1	3.5	0.032	12.6	12.2	239
	LFP (HE)	301.7	58.6	1282	0.5	19.0	1.1	0.040	16.8	13.4	278
Using water as solvent instead of NMP	NCA (HE)	366.2	49.1	1708	0.4	24.6	3.4	0.029	12.8	11.6	243
	NMC532 (HE)	502.2	66.5	2193	0.6	32.3	5.0	0.039	17.8	15.9	339
	NMC622 (HE)	508.5	66.1	2223	0.5	32.0	5.2	0.038	17.0	15.7	329
	NMC811 (HE)	387.6	51.3	1729	0.4	26.1	3.7	0.031	13.7	12.1	259
	NMC900 (HE)	330.8	43.9	1493	0.4	23.0	3.1	0.028	12.1	10.4	227
	LFP (HE)	208.3	40.2	1119	0.4	18.9	0.4	0.032	16.1	10.7	260

		Cumulative Energy Demand (CED) [kWh/kWh]	Global Warming Potential (GWP) [$kgCO_2$-eq/kWh]	Terrestrial Ecotoxicity Potential (TEP) [kg1.4DCB-eq/kWh]	Terrestrial Acidification Potential (TAP) [$kgSO_2$-eq/kWh]	Surplus Ore Potential (SOP) [kgCu-eq/kWh]	Water Consumption Potential (WCP) [m^3/kWh]	Freshwater Eutrophication Potential (FEP) [kg P-eq/kWh]	Freshwater Ecotoxicity Potential (FEtP) [kg1.4DCB-eq/kWh]	Human toxicity, cancer (HTPc) [kg1.4DCB-eq/kWh]	Human toxicity, non-cancer (HTPnc) [kg1.4DCB-eq/kWh]
larger cells, with thinner walls, made of aluminium	NCA (HE)	431.2	63.8	1807	0.5	24.7	3.8	0.033	13.4	13.9	255
	NMC532 (HE)	591.5	86.5	2334	0.6	32.6	5.6	0.045	18.5	19.2	356
	NMC622 (HE)	592.9	85.1	2356	0.6	32.1	5.8	0.043	17.7	18.7	345
	NMC811 (HE)	457.7	67.0	1840	0.5	26.2	4.2	0.035	14.3	14.6	273
	NMC900 (HE)	394.2	58.1	1594	0.4	23.1	3.5	0.031	12.7	12.6	239
	LFP (HE)	303.1	61.6	1265	0.5	19.0	1.0	0.038	16.9	14.2	278
coated NCA, coated NMC, coated LFP	NCA (HE)	427.0	62.3	1819	0.5	24.7	3.8	0.033	13.3	13.3	253
	NMC532 (HE)	586.6	84.8	2348	0.6	32.6	5.6	0.044	18.4	18.4	354
	NMC622 (HE)	588.2	83.4	2370	0.6	32.2	5.8	0.043	17.6	18.0	343
	NMC811 (HE)	453.9	65.6	1851	0.5	26.3	4.2	0.035	14.2	14.0	271
	NMC900 (HE)	390.9	56.9	1604	0.4	23.1	3.5	0.031	12.6	12.1	238
	LFP (HE)	300.3	59.8	1282	0.5	19.0	1.0	0.038	16.8	13.3	276
Modified anode material mix for dry coating	NCA (HE)	425.7	62.6	1821	0.5	25.5	3.8	0.033	13.3	13.3	254
	NMC532 (HE)	583.8	84.7	2349	0.6	33.3	5.6	0.044	18.4	18.5	355
	NMC622 (HE)	585.9	83.4	2371	0.6	32.9	5.8	0.043	17.6	18.0	344
	NMC811 (HE)	453.6	66.0	1860	0.5	26.8	4.2	0.035	14.2	14.1	272
	NMC900 (HE)	391.8	57.4	1617	0.4	23.6	3.5	0.031	12.6	12.2	239
	LFP (HE)	293.1	59.2	1282	0.5	19.9	1.0	0.038	16.8	13.3	277

Ongoing optimization trends

Improved scenario** (absolute)	NCA (HE)	374.0	49.9	1607	0.4	24.5	3.4	0.027	9.8	11.2	197
	NMC532 (HE)	515.7	67.8	2059	0.5	32.1	5.1	0.037	13.5	15.4	276
	NMC622 (HE)	519.9	67.1	2097	0.5	31.8	5.3	0.036	13.1	15.2	271
	NMC811 (HE)	395.9	51.9	1623	0.4	26.0	3.8	0.029	10.4	11.6	211
	NMC900 (HE)	337.7	44.3	1397	0.4	22.9	3.1	0.025	9.1	9.9	183
	LFP (HE)	188.3	36.7	923	0.4	18.6	0.4	0.026	10.5	9.4	173
*Improved scenario** (relative)*	*NCA (HE)*	*-12.4%*	*-19.9%*	*-11.7%*	*-12.9%*	*-0.9%*	*-9.3%*	*-17.3%*	*-26.4%*	*-15.9%*	*-22.2%*
	NMC532 (HE)	*-11.6%*	*-19.4%*	*-12.2%*	*-14.0%*	*-0.9%*	*-8.4%*	*-17.0%*	*-26.5%*	*-15.6%*	*-22.0%*
	NMC622 (HE)	*-11.5%*	*-19.4%*	*-11.5%*	*-13.4%*	*-0.9%*	*-8.0%*	*-16.8%*	*-25.6%*	*-15.6%*	*-21.0%*
	NMC811 (HE)	*-12.7%*	*-20.8%*	*-12.3%*	*-13.8%*	*-0.9%*	*-9.2%*	*-17.5%*	*-26.6%*	*-17.0%*	*-22.3%*
	NMC900 (HE)	*-13.5%*	*-21.9%*	*-12.8%*	*-14.3%*	*-0.9%*	*-10.1%*	*-18.1%*	*-27.2%*	*-18.0%*	*-23.1%*
	LFP (HE)	*-36.5%*	*-38.1%*	*-28.0%*	*-24.3%*	*-2.4%*	*-59.7%*	*-31.8%*	*-37.6%*	*-29.0%*	*-37.0%*

FIGURE 8 Effect of improvements in cell design and technology on the environmental impact of different lithium-ion battery (LIB) chemistries, in high-energy (HE) configuration. *Improvements in production technology are obtained from Degen (2023) and Degen et al. (2023). **For NCA (nickel–cobalt–aluminum) and NMC (nickel–manganese–cobalt), we assume N-methyl-2-pyrrolidone (NMP) as solvent; for LFP (lithium–iron–phosphate), we assume water as solvent. The underlying assumptions are given in Section 2. The results for high-power (HP) configurations can be found in Supplement S4. The calculations can be found in Supplement S3.

3.4 | Short-term optimization potential and ongoing trends

The results of the aforementioned analyses are subject to a number of uncertainties and ongoing optimization efforts. For example, the NMP is reconditioned and reused in modern gigafactories. This has the potential to reduce the environmental footprint of the NMP but requires significant initial investments in equipment. However, to date, there are still numerous battery cell factories in operation, particularly in Asia, which do not recondition and reuse NMP. In the case of LFP chemistries, industrial approaches are also being considered that utilize water as a solvent. Furthermore, efforts are being made to reduce the thickness of the current collectors (aluminum foil and copper foil) to increase the energy density of the battery cells (Link et al., 2023). Given the high cost of energy, particularly for natural gas in Europe, battery cell factories are also being optimized in terms of energy (Degen et al., 2023; Schütte et al., 2024). This has resulted in a transition from natural gas to electricity as an energy source. Furthermore, cell casings are becoming larger, with thinner casing walls made of aluminum; NCA, NMC, and LFP active materials are being coated; and dry coating is being applied in anode production (Taylor, 2022). Figure 8 shows how this affects the environmental impact of the various battery cell chemistries (in HE configuration). Figure 8 illustrates the impact of these changes on the environmental footprint of the various battery cell chemistries (in HE configuration). In this analysis, we focus on the impact on LIB cells, excluding SIB and SSB cells, as these are not yet in widespread production and are unlikely to be in the near future. The results for HP configurations can be found in Supplement S4. The assumptions made are explained in Supporting Information S1.

Figure 8 illustrates that trends such as NMP recycling, reducing the thickness of the current collector, optimizing LIB factory production, and using water as a solvent have a favorable impact on the environmental damage potential of battery cells. Conversely, other trends, including the transition from natural gas to electricity, utilizing lighter and larger casings made of aluminum, coated active material, and dry coating, have an adverse effect on the environmental damage potential of battery cells. However, the negative impact of electricity generation is primarily attributable to the fact that the current electricity mix is still derived from a significant proportion of fossil fuels. Nevertheless, this is anticipated to decline further, reaching a point where the kWh of electricity is expected to have a lower environmental impact than natural gas. The use of lighter cell casings can lead to reduced energy consumption during the operational phase of an EV. Additionally, the coating of CAMs has the potential to enhance battery performance and extend its lifespan.

The combination of various trends shows that the damage potential can be notably reduced overall, with a reduction of between approximately −1% (SOP of NMC and NCA) and −54% (WCP of LFP). The overall damage potential of LFP cells can be reduced the most in percentage terms by the ongoing development trends.

4 | DISCUSSION AND CONCLUSION

The objective of this study was to identify the environmental impact of LIB cell types currently and in the near future employed in the automotive industry. The following findings were established:

First, the production of an LIB cell necessitates the utilization of approximately ~296–624 kWh_{CED}/kWh_{cell} of primary energy with GHG emissions of approximately ~57–92 $kgCO_2$-eq/kWh_{cell}. These figures are contingent upon the specific cell chemistry employed. The GWP of NMC811 in an HE configuration is found to be approximately ~66 $kgCO_2$-eq/kWh_{cell}, while in an HP configuration, it is approximately ~72 $kgCO_2$-eq/kWh_{cell}. This is notably less than the figures indicated in current literature sources (Crenna et al., 2021; Kallitsis et al., 2020). For example, Crenna et al. report GWPs between 110 and 120 $kgCO_2$-eq/kWh_{cell} for NMC811 (Crenna et al., 2021). Kallitsis report a GWP of 140 $kgCO_2$-eq/kWh_{cell} for NMC811 (Kallitsis et al., 2020). In contrast, Winjobi et al. report notably lower GWP values between 50 and 70 $kgCO_2$-eq/kWh_{cell} for NMC811 (Winjobi et al., 2022). Our study has confirmed the existence of such low GWPs.

Second, with regard to the environmental impact of an LIB cell, a notable distinction can be observed between cells constructed in an HE configuration, characterized by a thicker coating, and those built in an HP configuration, which feature a thinner coating. This phenomenon is evident across all impact categories. For instance, the HP configuration has been found to exhibit a GWP that is approximately 10%–20% higher than that of the respective HE configuration. This illustrates the pivotal role that the construction of a battery cell plays in determining its environmental impact. The mere specification of the cathode chemistry (e.g., NMC111, NMC622, NMC811) is insufficient for an LCA study; the areal load of the electrode must always be provided.

Third, there are considerable differences in the environmental impact of NMC chemistries, depending on the specific type of NMC employed. For instance, NMC900 has a GWP that is approximately 33% lower than that of NMC532. The existing LCA studies, which analyze a range of NMC chemistries, also arrive at disparate conclusions in this regard. Crenna et al. and Llamas-Orozco et al. do not identify any significant differences between different NMC chemistries (Crenna et al., 2021; Llamas-Orozco et al., 2023). Winjobi et al. (2022) report a slight reduction in the impact criteria with an increasing nickel content and thus a reduced cobalt content and increased energy density (Winjobi et al., 2022). In contrast, Kallitsis et al. (2020) clearly point to this effect. The findings of this study corroborate the notion that the environmental impact of battery cells can be mitigated by reducing the cobalt content and increasing the nickel content in NMC cells. This phenomenon can be attributed to two key factors: first, nickel is less detrimental to the environment than cobalt, and second, an elevated nickel share also leads to an enhancement in the energy density of the cell. Consequently, the environmental impact of passive materials (e.g., casing, current collectors, especially copper foil) and overhead (e.g., energy costs in cell production) is reduced in an "impact per kWh_{cell}" calculation.

Fourth, the key contributors to environmental damage in LIB cells are $CoSO_4$, copper foil, and NMP as a solvent. It is already known that $CoSO_4$ has a high damage potential. However, the fact that copper in the battery cell has a high damage potential only becomes apparent when other damage categories than GWP or CED are analyzed. This has been previously investigated by Kallitsis et al. in a comprehensive manner (Kallitsis et al., 2020). They also highlight the significant detrimental impact of copper in battery cells. Copper is one of the most harmful materials per kilogram in a battery cell, with strong damage potential in almost all impact categories. Additionally, it has a high mass share per kWh_{cell}, ranging from two to four times that of lithium. The high specific damage potential of copper in combination with its high mass share makes copper an environmentally critical component in a battery cell. Furthermore, the major effect of NMP has not been recognized or named in the latest and relevant studies (Gutsch & Leker, 2024; Winjobi et al., 2022). This may be due to the fact that NMP is only an auxiliary material that is not contained in the final battery cell and therefore not taken into account in the BOM (Gutsch & Leker, 2024). Other studies name NMP but argue that it is recycled and thus not further focused (Kallitsis et al., 2020). Although NMP is usually recycled in new, large battery cell factories, in older, existing factories, new NMP is usually used. This results in a correspondingly higher damage potential of the battery cells. In short, our findings demonstrate that the significant influence of copper and NMP is not adequately considered in many LCA studies of battery cells.

Fifth, the input materials for LFP active material have much lower damage potential than CAMs with nickel and cobalt components (NMC and NCA). The GWP for the synthesis of LFP is 11.6 $kgCO_2$-eq/kg, while it is double as high for NMC900 with 26.4 $kgCO_2$-eq/kg. However, at the level of individual cells, LFP has a slightly higher GWP than NMC900. This indicates that NMC900 is the chemistry with the lowest GWP at the level of individual cells across the entire range of cell types analyzed. These results do not corroborate those of Llamas-Orozco et al., who found that the GWP of LFP chemistry was approximately 30% lower than that of NMC and NCA cells (Llamas-Orozco et al., 2023). Our findings also highlight the crucial role of energy density in understanding the environmental impact of battery cells. High energy densities can offset high environmental impacts by increasing the overall ratio of energy density to the environmental impact of the battery cell.

Sixth, the SIB cell that we have analyzed (NaNFM442) has the lowest environmental impact in a number of impact categories. This is due to the fact that NaNFM442 does not utilize any cobalt, copper, or graphite. However, in the relevant impact category of climate change, the GWP of

NaNFM422 is situated between that of NMC811 and NMC622. A GWP of 75–87 $kgCO_2$- eq/kWh_{cell} is calculated for NaNFM442. In the literature, the values presented vary considerably. Peters et al. (2016) report a GWP of 140 $kgCO_2$-eq/kWh_{cell} for an SIB cell with NMMT (sodium nickel manganese magnesium titanate oxide) chemistry (Peters et al., 2016). This value is almost twice as high as the GWP calculated in this study. Schneider et al. (2019) report GWPs of 80–150 $kgCO_2$-eq/kWh_{cell}, which is also higher than the values calculated in this study. In the most comprehensive LCA study on SIBs to date, also by Peters et al., five different SIBs are analyzed and GWPs between 50 and 90 $kgCO_2$-eq/kWh_{cell} are determined, which is in a similar range to our results (Peters et al., 2021). However, the cell chemistry NaNFM442 used by us was not included in the analysis by Peters et al. Despite this, Peters et al. (2016) also concluded that SIB cells have a higher GWP than LIB cells. However, in their study, NMC622 reference cells exhibited a lower GWP than LFP reference cells. Our findings challenge this conclusion.

Seventh, SSB cells have in many categories a similar or slightly increased environmental impact like NMC and NCA cells, except for SOP. The main driver for an increased impact of SSB cells is the use of lithium (metal) on the anode side, which has a much higher environmental impact than graphite. Most of the other components of the cell remain the same, except for the electrolyte. However, the solid electrolyte has a negligible mass share in the cell and also a low specific damage potential, as demonstrated in our study. We calculate a GWP of between 88 and 130 $kgCO_2$-eq/kWh_{cell} for NMC900 cells with an oxidic solid electrolyte. The few existing literature sources provide values of up to ~18,000 $kgCO_2$-eq/kWh_{cell} (Troy et al., 2016) and ~33,000 $kgCO_2$- eq/kWh_{cell} (Zhang et al., 2022). However, these were determined by analyzing SSB coin cells. Our calculations demonstrate that the environmental impacts of larger SSB cells are comparable to those of LIB cells. It is also important to note that the high thickness of the lithium metal layer (20 µm) is primarily a result of production handling considerations, rather than electrochemical factors. From an electrochemical perspective, the lithium layer could be as thin as a few micrometers. However, the reliable large-scale production of such a thin layer is currently challenging. Therefore, by improving lithium processing and reducing the anode thickness, it is possible to significantly reduce the environmental impact of SSB cells.

Eighth, there are trends toward optimizing cell designs and production. These are not necessarily intended to reduce environmental impacts but may nevertheless lead to a reduction in these. For instance, trends include optimizing cell designs (e.g., reducing the thickness of the copper foil, increasing the cell casing) (Link et al., 2023), recycling (reconditioning of NMP; Nurjanah et al., 2023), and improving production technology (Degen et al., 2023). The results demonstrate that ongoing developments in cell design and production have the potential to reduce the damage potential of LIB cells by −19% for NMC532 and −38% for LFP. This finding is one of the most significant insights of the study, as it highlights the significant optimization potential of battery cells with regard to their ecological impacts. The GWP of NMC900 cells can be reduced by −22% to ~44 $kgCO_2$-eq/kWh_{cell}, and the GWP of LFP cells can be reduced by −38% to ~37 $kgCO_2$-eq/kWh_{cell}. It should be noted that these figures do not take into account the recycling of nickel, cobalt, lithium, copper, etc. This will likely also affect the environmental impact within the next years.

This study is accompanied by its limitations. We present the environmental footprint of all major battery cells for EVs, but the analysis is limited from cradle to gate. We do not take into account the subsequent use phase or the final recycling phase. However, the main proportion of GHG emissions from EVs is not solely emitted during their production, but also during their use. Here, in addition to the application scenario, the local energy mix and the weight of the EVs are of major importance. The greater the weight of an EV, the greater the energy expenditure per unit distance traveled. This implies that a heavy battery is more disadvantageous than a light battery with the same energy content. In concrete terms, this implies that an LFP battery cell (low gravimetric energy density) in a cradle-to-grave approach may be more environmentally disadvantageous than an SSB battery cell (high gravimetric energy density), although in our cradle-to-gate approach, the LFP cell has a notably lower damage potential than the SSB cell. On the other hand, LFP cells have a longer lifetime than NMC and NCA cells, which also would affect the environmental footprint when including the use phase. However, as previously stated, this depends on the specific scenario. The data obtained and presented in this study can serve as a foundation for further research and analysis by other scholars in the field.

Furthermore, our study does not consider the recycling and reuse of the most critical raw materials, including lithium, nickel, cobalt, manganese, aluminum, copper, graphite, and others. The rates of recycling are determined by legislative bodies, as exemplified by the EU Battery Regulation (Official Journal of the European Union 2023), which was implemented across all EU countries at the beginning of 2024. The recycling of these materials will have a notable impact on the ecological impact factor of the materials in question, which in turn will have an effect on the calculated values. However, the quantitative change depends largely on the specific scenario, such as the recycling technology used, its efficiency, the energy mix, and many more. The data obtained and provided in our study can be used by other researchers as a basis for calculations and studies.

ACKNOWLEDGMENTS

This research was funded by the German Federal Ministry of Education and Research (grant number 03XP0256). We would like to thank all experts who participated in the assessment.

Open access funding enabled and organized by Projekt DEAL.

CONFLICT OF INTEREST STATEMENT

The authors declare no conflicts of interest.

DATA AVAILABILITY STATEMENT

The data that supports the findings of this study are available in the supporting information of this article (supporting information S1-S4). What kind of data is found in these is described in the section "supporting information" at the end of this document. A further, more detailed documentation of the data structure can be found in the "read me" sections in the supplementary information itself.

ORCID


Florian Degen https://orcid.org/0000-0003-3650-1803

REFERENCES

A2Mac1. (2023). Benchmarking data and tear-down reports. A2MAC1, Belleville, MI. https://www.a2mac1.com/

Ahmed, S., Nelson, P. A., Gallagher, K. G., & Dees, D. W. (2016). Energy impact of cathode drying and solvent recovery during lithium-ion battery manufacturing. *Journal of Power Sources*, *322*, 169–78. https://doi.org/10.1016/j.jpowsour.2016.04.102

Ambrose, H., & Kendall, A. (2016). Effects of battery chemistry and performance on the life cycle greenhouse gas intensity of electric mobility. *Transportation Research Part D: Transport and Environment*, *47*, 182–94. https://doi.org/10.1016/j.trd.2016.05.009

B3 Corporation. (2015). *LIB materials market bulletin E15Q3—Market reports*. B3 Corporation, Tokyo, Japan.

Bawankar, S., Dwivedi, G., Nanda, I., Daniel Jiménez Macedo, V., Kesharvani, S., Meshram, K., Jain, S., Mishra, S., Pratap Singh, V., & Verma, P. (2023). Environmental impact assessment of lithium ion battery employing cradle to grave. *Sustainable Energy Technologies and Assessments*, *60*, 103530. https://doi.org/10.1016/j.seta.2023.103530

Bhandari, N. B., Cai, A., Yuzawa, K., Zhang, J., Joshi, V., Fang, F., Lee, G., Harada, R., & Shin, S. (2022). Batteries: The greenflation challenge. https://www.goldmansachs.com/insights/pages/gs-research/batteries-the-greenflation-challenge/report.pdf

Crenna, E., Gauch, M., Widmer, R., Wäger, P., & Hischier, R. (2021). Towards more flexibility and transparency in life cycle inventories for lithium-ion batteries. *Resources, Conservation and Recycling*, *170*, 105619. https://doi.org/10.1016/j.resconrec.2021.105619

Cusenza, M. A., Bobba, S., Ardente, F., Cellura, M., & Di Persio, F. (2019). Energy and environmental assessment of a traction lithium-ion battery pack for plug-in hybrid electric vehicles. *Journal of Cleaner Production*, *215*, 634–49. https://doi.org/10.1016/j.jclepro.2019.01.056

Dai, Q., Kelly, J. C., Dunn, J. B., & Benavides, P. (2018). *Update of bill-of-materials and cathode materials production for lithium-ion batteries in the GREET model*. Argonne National Laboratory.

Dai, Q., Kelly, J. C., Gaines, L., & Wang, M. (2019). Life cycle analysis of lithium-ion batteries for automotive applications. *Batteries*, *5*(2), 48. https://doi.org/10.3390/batteries5020048

Degen, F. (2023). Lithium-ion battery cell production in Europe: Scenarios for reducing energy consumption and greenhouse gas emissions until 2030. *Journal of Industrial Ecology*, *27*(3), 964–76. https://doi.org/10.1111/jiec.13386

Degen, F., & Schütte, M. (2022). Life cycle assessment of the energy consumption and GHG emissions of state-of-the-art automotive battery cell production. *Journal of Cleaner Production*, *330*, 129798. https://doi.org/10.1016/j.jclepro.2021.129798

Degen, F., Winter, M., Bendig, D., & Tübke, J. (2023). Energy consumption of current and future production of lithium-ion and post lithium-ion battery cells. *Nature Energy*, *8*, 1284–1295. https://doi.org/10.1038/s41560-023-01355-z

Deng, Y., Li, J., Li, T., Gao, X., & Yuan, C. (2017). Life cycle assessment of lithium sulfur battery for electric vehicles. *Journal of Power Sources*, *343*, 284–95. https://doi.org/10.1016/j.jpowsour.2017.01.036

Ding, Y., Cano, Z. P., Yu, A., Lu, J., & Chen, Z. (2019). Automotive Li-ion batteries: Current status and future perspectives. *Electrochemical Energy Reviews*, *2*(1), 1–28. https://doi.org/10.1007/s41918-018-0022-z

Dunn, J. B., James, C., Gaines, L., Gallagher, K., Dai, Q., & Kelly, J. C. (2015). *Material and energy flows in the production of cathode and anode materials for lithium ion batteries ANL/ESD-14/10 Rev*. Argonne National Laboratory.

Ellingsen, L. A.-W., Majeau-Bettez, G., Singh, B., Srivastava, A. K., Valøen, L. O., & Strømman, A. H. (2014). Life cycle assessment of a lithium-ion battery vehicle pack. *J of Industrial Ecology*, *18*(1), 113–24. https://doi.org/10.1111/jiec.12072

Engels, P., Cerdas, F., Dettmer, T., Frey, C., Hentschel, J., Herrmann, C., Mirfabrikikar, T., & Schueler, M. (2022). Life cycle assessment of natural graphite production for lithium-ion battery anodes based on industrial primary data. *Journal of Cleaner Production*, *336*, 130474. https://doi.org/10.1016/j.jclepro.2022.130474

Faria, R., Marques, P., Garcia, R., Moura, P., Freire, F., Delgado, J., & de Almeida, A. T. (2014). Primary and secondary use of electric mobility batteries from a life cycle perspective. *Journal of Power Sources*, *262*, 169–77. https://doi.org/10.1016/j.jpowsour.2014.03.092

Fleischmann, J., Hanicke, M., Horetsky, E., Ibrahim, D., Jautelat, S., Linder, M., Schaufuss, P., Torscht, L., & van de Rijt, A. (2023). *Battery 2030: Resilient, sustainable, and circular*. McKinsey & Company.

Fraunhofer Institute for Systems and Innovation Research ISI. (2023). Meta-market-monitoring: Interactive databases of the battery value chain. https://metamarketmonitoring.de/en/

Gutsch, M., & Leker, J. (2024). Costs, carbon footprint, and environmental impacts of lithium-ion batteries—From cathode active material synthesis to cell manufacturing and recycling. *Applied Energy*, *353*, 122132. https://doi.org/10.1016/j.apenergy.2023.122132

Huijbregts, M., Steinmann, Z., Elshout, P., Stam, G., Verones, F., Vieira, M., Hollander, A., Zijp, M., & van Zelm, R. (2016). ReCiPe 2016 v1.1: A harmonized life cycle impact assessment method at midpoint and endpoint level RIVM Report 2016-0104a. https://pre-sustainability.com/legacy/download/Report_ReCiPe_2017.pdf

IEA, International Energy Agency. (2023a). Energy Technology Perspectives 2023. Paris. https://www.iea.org/reports/energy-technology-perspectives-2023

IEA, International Energy Agency. (2023b). Global EV Outlook 2023: Catching up with climate ambitions. Paris. https://www.iea.org/reports/global-ev-outlook-2023

Jenu, S., Deviatkin, I., Hentunen, A., Myllysilta, M., Viik, S., & Pihlatie, M. (2020). Reducing the climate change impacts of lithium-ion batteries by their cautious management through integration of stress factors and life cycle assessment. *Journal of Energy Storage*, *27*, 101023. https://doi.org/10.1016/j.est.2019.101023

Kallitsis, E. (2022). On the energy use of battery Gigafactories. *Journal of Cleaner Production*, *364*, 132573. https://doi.org/10.1016/j.jclepro.2022.132573

Kallitsis, E., Korre, A., Kelsall, G., Kupfersberger, M., & Nie, Z. (2020). Environmental life cycle assessment of the production in China of lithium-ion batteries with nickel-cobalt-manganese cathodes utilising novel electrode chemistries. *Journal of Cleaner Production*, *254*, 120067. https://doi.org/10.1016/j.jclepro.2020.120067

Keshavarzmohammadian, A., Cook, S. M., & Milford, J. B. (2018). Cradle-to-gate environmental impacts of sulfur-based solid-state lithium batteries for electric vehicle applications. *Journal of Cleaner Production*, *202*, 770–78. https://doi.org/10.1016/j.jclepro.2018.08.168

Kim, H. C., Wallington, T. J., Arsenault, R., Bae, C., Ahn, S., & Lee, J. (2016). Cradle-to-gate emissions from a commercial electric vehicle Li-ion battery: A comparative analysis. *Environmental Science & Technology*, *50*(14), 7715–22. https://doi.org/10.1021/acs.est.6b00830

Lain, Brandon, & Kendrick (2019). Design strategies for high power vs. high energy lithium ion cells. *Batteries*, *5*(4), 64. https://doi.org/10.3390/batteries5040064

Lastoskie, C. M., & Dai, Q. (2015). Comparative life cycle assessment of laminated and vacuum vapor-deposited thin film solid-state batteries. *Journal of Cleaner Production*, *91*, 158–69. https://doi.org/10.1016/j.jclepro.2014.12.003

Le Varlet, T., Schmidt, O., Gambhir, A., Few, S., & Staffell, I. (2020). Comparative life cycle assessment of lithium-ion battery chemistries for residential storage. *Journal of Energy Storage*, *28*, 101230. https://doi.org/10.1016/j.est.2020.101230

Link, S., Neef, C., & Wicke, T. (2023). Trends in automotive battery cell design: A statistical analysis of empirical data. *Batteries*, *9*(5), 261. https://doi.org/10.3390/batteries9050261

Llamas-Orozco, J. A., Meng, F., Walker, G. S., Abdul-Manan, A. F. N., MacLean, H. L., Posen, I. D., & McKechnie, J. (2023). Estimating the environmental impacts of global lithium-ion battery supply chain: A temporal, geographical, and technological perspective. *PNAS Nexus*, *2*(11), pgad361. https://doi.org/10.1093/pnasnexus/pgad361

Majeau-Bettez, G., Hawkins, T. R., & Strømman, A. H. (2011). Life cycle environmental assessment of lithium-ion and nickel metal hydride batteries for plug-in hybrid and battery electric vehicles. *Environmental Science & Technology*, *45*(10), 4548–54. https://doi.org/10.1021/es103607c

Mandade, P., Weil, M., Baumann, M., & Wei, Z. (2023). Environmental life cycle assessment of emerging solid-state batteries: A review. *Chemical Engineering Journal Advances*, *13*, 100439. https://doi.org/10.1016/j.ceja.2022.100439

Marques, P., Garcia, R., Kulay, L., & Freire, F. (2019). Comparative life cycle assessment of lithium-ion batteries for electric vehicles addressing capacity fade. *Journal of Cleaner Production*, *229*, 787–94. https://doi.org/10.1016/j.jclepro.2019.05.026

Masias, A., Marcicki, J., & Paxton, W. A. (2021). Opportunities and challenges of lithium ion batteries in automotive applications. *ACS Energy Letters*, *6*(2), 621–30. https://doi.org/10.1021/acsenergylett.0c02584

Notter, D. A., Gauch, M., Widmer, R., Wäger, P., Stamp, A., Zah, R., & Althaus, H.-J. (2010). Contribution of Li-ion batteries to the environmental impact of electric vehicles. *Environmental Science & Technology*, *44*(17), 6550–56. https://doi.org/10.1021/es903729a

Nurjanah, I., Hsieh, L.-H. C., Chiang, Y.-H., & Sean, W.-Y. (2023). Energy saving in NMP (N- methyl-2-pyrrolidone) recovery process by numerical modeling. *Environmental Technology & Innovation*, *31*, 103218. https://doi.org/10.1016/j.eti.2023.103218

Peters, J., Buchholz, D., Passerini, S., & Weil, M. (2016). Life cycle assessment of sodium-ion batteries. *Energy & Environmental Science*, *9*(5), 1744–51. https://doi.org/10.1039/C6EE00640J

Peters, J. F., Baumann, M., Binder, J. R., & Weil, M. (2021). On the environmental competitiveness of sodium-ion batteries under a full life cycle perspective—A cell-chemistry specific modelling approach. *Sustainable Energy Fuels*, *5*(24), 6414–29. https://doi.org/10.1039/D1SE01292D

Qian, L., Li, T., Dong, X., & Li, S. (2023). Life cycle assessment of high nickel ternary lithium (NCM811) power batteries. *International Journal of Green Energy*, *21*(8), 1897–1909. https://doi.org/10.1080/15435075.2023.2276162

Quinn, J. B., Waldmann, T., Richter, K., Kasper, M., & Wohlfahrt-Mehrens, M. (2018). Energy density of cylindrical Li-ion cells: A comparison of commercial 18650 to the 21700 cells. *Journal of the Electrochemical Society*, *165*(14), A3284–A3291. https://doi.org/10.1149/2.0281814jes

Rauscher, S. (2014). *Einfluss von material- und beschichtungsparametern auf die elektrodenmorphologie und die leistungsparameter von lithiumionen-zellen*. Universität Ulm.

REGULATION (EU) 2023/1542 OF THE EUROPEAN PARLIAMENT AND OF THE COUNCIL. Regulation (EU) 2023/1542 of the European Parliament and of the Council of July 12 concerning batteries and waste batteries, amending Directive 2008/98/EC and Regulation (EU) 2019/1020 and repealing Directive 2006/66/EC. Official Journal of the European Union. https://eur-lex.europa.eu/legal-content/EN/TXT/PDF/?uri=CELEX:32023R1542

Rolinck, M., Khakmardan, S., Cerdas, F., Mennenga, M., Li, W., & Herrmann, C. (2023). Completeness evaluation of LCI datasets for the environmental assessment of lithium compound production scenarios. *Procedia CIRP*, *116*, 726–31. https://doi.org/10.1016/j.procir.2023.02.122

Schmaltz, T., Wicke, T., Weymann, L., Voß, P., Neef, C., & Thielmann, A. (2022). *Solid-state battery roadmap 2035+*. https://www.isi.fraunhofer.de/content/dam/isi/dokumente/cct/2022/SSB_Roadmap.pdf

">Schneider, S. F., Bauer, C., Novák, P., & Berg, E. J. (2019). A modeling framework to assess specific energy, costs and environmental impacts of Li-ion and Na-ion batteries. *Sustainable Energy Fuels*, *3*(11), 3061–70. https://doi.org/10.1039/C9SE00427K

Schütte, M., Degen, F., & Walter, H. (2024). Reducing energy consumption and greenhouse gas emissions of industrial drying processes in lithium-ion battery cell production: A qualitative technology benchmark. *Batteries*, *10*(2), 64. https://doi.org/10.3390/batteries10020064

Shen, K., Zhai, Q., Gu, Y., Wang, W., Cao, H., Hauschild, M., & Yuan, C. (2023). Life cycle assessment of lithium ion battery from water-based manufacturing for electric vehicles. *Resources, Conservation and Recycling*, *198*, 107152. https://doi.org/10.1016/j.resconrec.2023.107152

Smith, L., Ibn-Mohammed, T., Astudillo, D., Brown, S., Reaney, I. M., & Koh, S. C. L. (2021). The role of cycle life on the environmental impact of Li 6.4 La 3 Zr 1.4 Ta 0.6 O 12 based solid-state batteries. *Advanced Sustainable Systems*, *5*(2), 2000241. https://doi.org/10.1002/adsu.202000241

Sun, X., Luo, X., Zhang, Z., Meng, F., & Yang, J. (2020). Life cycle assessment of lithium nickel cobalt manganese oxide (NCM) batteries for electric passenger vehicles. *Journal of Cleaner Production*, *273*, 123006. https://doi.org/10.1016/j.jclepro.2020.123006

Taylor, N. (2022). *Tesla 4680 cell*. https://www.batterydesign.net/tesla-4680-cell/

Troy, S., Schreiber, A., Reppert, T., Gehrke, H.-G., Finsterbusch, M., Uhlenbruck, S., & Stenzel, P. (2016). Life cycle assessment and resource analysis of all-solid-state batteries. *Applied Energy*, *169*, 757–67. https://doi.org/10.1016/j.apenergy.2016.02.064

Winjobi, O., Kelly, J. C., & Dai, Q. (2022). Life-cycle analysis, by global region, of automotive lithium-ion nickel manganese cobalt batteries of varying nickel content. *Sustainable Materials and Technologies*, *32*, e00415. https://doi.org/10.1016/j.susmat.2022.e00415

Zackrisson, M., Avellán, L., & Orlenius, J. (2010). Life cycle assessment of lithium-ion batteries for plug-in hybrid electric vehicles—Critical issues. *Journal of Cleaner Production*, *18*(15), 1519–29. https://doi.org/10.1016/j.jclepro.2010.06.004

Zhang, J., Ke, X., Gu, Y., Wang, F., Zheng, D., Shen, K., & Yuan, C. (2022). Cradle-to-gate life cycle assessment of all-solid-state lithium-ion batteries for sustainable design and manufacturing. *International Journal of Life Cycle Assessment*, *27*(2), 227–37. https://doi.org/10.1007/s11367-022-02023-2

Zhao, S., & You, F. (2019). Comparative life-cycle assessment of Li-ion batteries through process-based and integrated hybrid approaches. *ACS Sustainable Chemistry and Engineering*, *7*(5), 5082–94. https://doi.org/10.1021/acssuschemeng.8b05902

SUPPORTING INFORMATION

Additional supporting information can be found online in the Supporting Information section at the end of this article.

How to cite this article: Degen, F., Mitterfellner, M., & Kampker, A. (2024). Comparative life cycle assessment of lithium-ion, sodium-ion, and solid-state battery cells for electric vehicles. *Journal of Industrial Ecology*, 1–16. https://doi.org/10.1111/jiec.13594